

Manipulation of Polymer Layer Characteristics by Electrochemical Polymerization from Mixtures of Aniline and *ortho*-Phenylenediamine Monomers

M. Kraljić Roković,¹ A. Jurišić,¹ M. Žic,¹ Lj. Duić,¹ Z. Schauperl²

¹Laboratory of Electrochemistry, Faculty of Chemical Engineering and Technology, University of Zagreb, Zagreb, Croatia

²Department of Materials, Faculty of Mechanical Engineering and Naval Architecture, University of Zagreb, Zagreb, Croatia

Received 2 June 2008; accepted 26 December 2008

DOI 10.1002/app.29974

Published online 19 March 2009 in Wiley InterScience (www.interscience.wiley.com).

ABSTRACT: The influence of adding *ortho*-phenylenediamine (OPDA) during the polymerization of aniline on the characteristics of the resulting polymer film was examined. When using a platinum electrode, the deposits were obtained from solutions containing 0.1 mol dm⁻³ aniline and 1, 5, or 10 mmol dm⁻³ OPDA. The deposits were also prepared from solutions containing 0.5 mol dm⁻³ aniline and 5, 10, or 50 mmol dm⁻³ OPDA. In both cases, 3 mol dm⁻³ phosphoric acid solution was used as a supporting electrolyte. The characteristics of the obtained layers were investigated through the catalytic effect of different polymer layers on hydroquinone/quinone (H₂Q/Q) test redox system. The results obtained confirm the earlier established catalytic effect on the potential of the redox reaction by shifting it to more reversible values. However, as the concentration of OPDA was increased, the resulting limiting current decreased, thus indicating in the presence of

OPDA a lower population of the available active centers necessary for the catalytic reaction to proceed. The influence of OPDA on polymer characteristics was also studied by using scanning electron microscopy as well as electrochemical impedance spectroscopy. The polymer was synthesized on a stainless steel electrode (13% Cr) from a solution containing 0.5 mol dm⁻³ aniline and 5, 10, or 50 mmol dm⁻³ OPDA. The layers were tested in chloride-containing solutions by monitoring the open circuit potential. The results obtained suggest that, by increasing the concentration of OPDA, the time of OCP in the passive region of stainless steel is prolonged. © 2009 Wiley Periodicals, Inc. *J Appl Polym Sci* 113: 427–436, 2009

Key words: modified polyaniline; conductive polymer; *ortho*-phenylenediamine; catalysis; corrosion protection; morphology

INTRODUCTION

Polyaniline (PANI) is one of the most investigated conducting polymers. It is a material interesting not only from the theoretical point of view in understanding and tailoring its conductive/nonconductive states but also from the practical point of view, because PANI is used in batteries as an active cathode material,¹ for corrosion protection,^{2–4} as a catalytic substrate for certain redox reactions,^{5,6} as a sensor electrode,^{7–9} etc.

This work also illustrates that the properties, as well as the morphology of PANI, could be tailored by polymerizing aniline from a mixture of aniline and certain aniline derivatives such as *ortho*-phenylenediamine (OPDA), *ortho*-methoxyaniline, *ortho*-ethoxyaniline, etc.^{10–14} Polymerization of aniline with the addition of OPDA revealed that, depending on the concentration of OPDA in the solution, the

sponge-like morphology in the case of pure PANI changes to a more compact layer as the concentration of OPDA increases.^{10,14} This change deserves to be studied, because it might result in the quality of PANI coating suitable for specific applications (e.g., in corrosion protection). Therefore, the aim of this work was to examine how the addition of OPDA in the aniline polymerization process changes the morphology of the PANI coating by making it more compact, which results in diminished catalytic currents of the chosen redox system, but on the other hand, increases the corrosion protection time of stainless steel (SS). Two different anilines, as well as different OPDA concentrations, were tested. The supporting electrolyte solution was 3 mol dm⁻³ H₃PO₄ because it was found especially suitable for polymer formation on the steel sample.⁴

MATERIALS AND METHODS

Two different substrates were used for working electrodes: (a) Pt-disc ($A = 0.07 \text{ cm}^2$), and (b) SS disc ($A = 0.95 \text{ cm}^2$). Voltammetric experiments were carried out by using a potentiostat (Wenking, LB75L;

Correspondence to: M. K. Roković (mkralj@fkit.hr).

Contract grant sponsor: Ministry of Science of the Republic of Croatia; contract grant number: 125-1252973-2576.

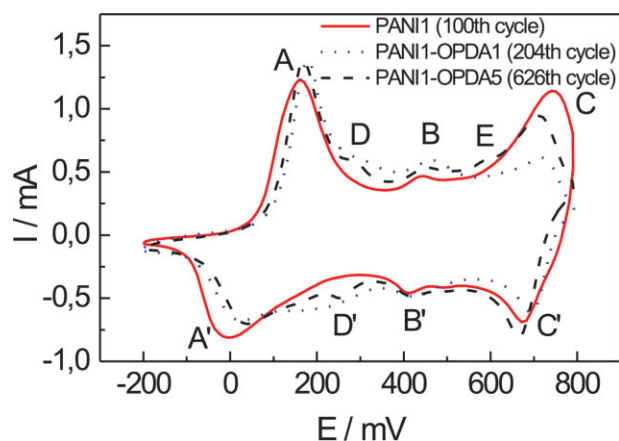


Figure 1 Cyclic voltammograms of PANI1 and PANI1-OPDA layer synthesis; $E_{\lambda} = 800$ mV, $c_{(\text{An})} = 0.1$ mol dm^{-3} . [Color figure can be viewed in the online issue, which is available at www.interscience.wiley.com.]

Bank Elektronik-Intelligent Controls GmbH, Pohlheim, Germany), a function generator (Wenking, VSG 83), and a PC for storing and evaluating the results.

The monomers were used as received: aniline (Kemika, Zagreb, Croatia) and OPDA (Sigma, Aldrich). The synthesis was always performed from 3 mol dm^{-3} H_3PO_4 supporting electrolyte solution in a standard one-compartment cell (Methrom) in an open-air atmosphere.

In Case (a), the counterelectrode was Pt-foil ($A = 1.5$ cm^2) and all the potentials were given against a saturated calomel electrode (SCE). The solutions used for the synthesis were as follows: (i) 0.1 mol dm^{-3} aniline (PANI1, PANI2) and 1 mmol dm^{-3} (OPDA1), 5 mmol dm^{-3} (OPDA5), or 10 mmol dm^{-3} (OPDA10) of OPDA; and (ii) 0.5 mol dm^{-3} aniline (PANI3, PANI4), and 5 mmol dm^{-3} (OPDA5), 10 mmol dm^{-3} (OPDA10), or 50 mmol dm^{-3} (OPDA50) of OPDA concentration. The method of synthesis was cyclic voltammetry (CV), employing the potential window between -200 and 800 mV (PANI1, PANI3) and between -200 and 1000 mV (PANI2, PANI4) at the scan rate of $v = 50$ mV s^{-1} .

The polymer layer growth was monitored by taking repetitive voltammograms, and the synthesis was monitored until the predetermined current of the first voltammetric current peak (current peak A, Fig. 1) reached the value of 1.4 mA.

The thicknesses of all polymer layers amount to ~ 0.85 μm . It was calculated from the amount of charge under the current peak A, necessary to switch from leucoemeraldine, the reduced form of PANI, to emeraldine, the oxidized form of PANI. The details describing the calculations and electrochemical reaction are given elsewhere.⁴ The thickness was calculated considering the PANI redox reaction only, because the charge representing the

redox reaction of poly-OPDA (current peak F) is negligible compared to PANI charge (Figs. 1 and 3).

The catalytic property of the resulting PANI-OPDA layer was tested for the quasi-reversible hydroquinone/quinone ($\text{H}_2\text{Q}/\text{Q}$) redox system, using voltammetry at rotating disc electrode (RDE). From a previous work,¹⁰ carried out in a chloride solution, it was known that the addition of OPDA into aniline solution for PANI synthesis resulted in the growth of layers with a decreased catalytic current compared to pure PANI layer. In this work, therefore, the study of the catalytic reaction serves only as a test of the influence of OPDA additions on the manipulation of active PANI sites available for the catalytic reaction. The concentration of H_2Q was 0.01 mol dm^{-3} /3 mol dm^{-3} H_3PO_4 , the potential window from 300 to 700 mV, scan rate $v = 2$ mV s^{-1} , and the rotation speed $\omega = 3000$ min^{-1} .

The electrochemical impedance spectroscopy (EIS) spectra of the layers were taken in 3 mol dm^{-3} H_3PO_4 using potentiostat (EG&G PAR Model 283; Oak Ridge, TN) and frequency response detector (EG&G PAR Model 1025). The superimposed sinusoidal voltage signal of 5 mV amplitude was applied. Data were collected within the frequency range of $10^5 - 10^{-2}$ Hz, taking five points per decade. The impedance data were analyzed by ZSimpWin fitting program.

In Case (b), the investigations using SS (13% Cr) as substrate were carried out using an SS disc mounted on a Teflon holder, a Pt-sheet as the counterelectrode ($A = 3$ cm^2), and Ag/AgCl (3 mol dm^{-3} KCl) as the reference electrode. The SS electrode was polished using 600-grit emery paper, washed with bi-distilled water and subsequently with ethanol. The synthesis of the polymer layer on SS was done by using CV by applying the potential scan within the potential window -400 to 1000 mV for a 0.5 mol dm^{-3} aniline solution (PANI) and with different concentrations of OPDA monomer (5, 10, or 50 mmol dm^{-3}) (PANI-OPDA5, PANI-OPDA10, and PANI-OPDA50).

The characteristics of the obtained polymer layers were tested through monitoring the open circuit potential (OCP) vs. time, using different test solutions (i.e., 0.1 mol dm^{-3} NaCl/3 mol dm^{-3} H_3PO_4 , and 0.1 mol dm^{-3} HCl). Prior to each OCP monitoring experiment, the electrode was polarized 1 min at 500 mV in the solution of pure supporting electrolyte (3 mol dm^{-3} H_3PO_4) to ensure the complete conversion of PANI into its conductive emeraldine (EM) form.

RESULTS AND DISCUSSION

Pt-electrode substrate

The results obtained by the CV method confirmed earlier voltammograms obtained when studying the same aniline/OPDA mixtures, but in HCl solutions

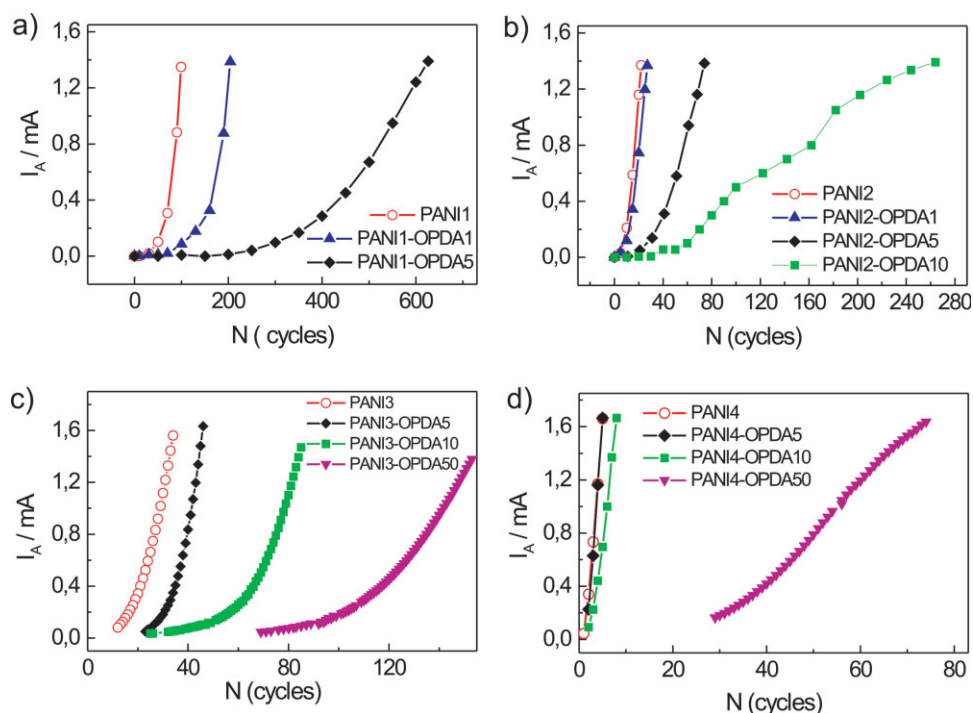


Figure 2 Current peak A (I_A) vs. number of cycles (N) for (a) PANI1 and PANI1-OPDA layers; $E_\lambda = 800$ mV, $c_{(\text{An})} = 0.1$ mol dm⁻³, (b) PANI2 and PANI2-OPDA layers; $E_\lambda = 1000$ mV, $c_{(\text{An})} = 0.1$ mol dm⁻³, (c) PANI3 and PANI3-OPDA layers; $E_\lambda = 800$ mV, $c_{(\text{An})} = 0.5$ mol dm⁻³, (d) PANI4 and PANI4-OPDA layers; $E_\lambda = 1000$ mV, $c_{(\text{An})} = 0.5$ mol dm⁻³. [Color figure can be viewed in the online issue, which is available at www.interscience.wiley.com.]

(Fig. 1).¹⁰ The shape of the voltammogram in Figure 1 indicates that, due to the addition of OPDA monomer, new current peaks (D/D' and E) develop besides those corresponding to PANI redox processes (A/A' and C/C'), representing leucoemeraldine/emeraldine (LE/EM) and emeraldine/ pernigraniline (EM/PG), respectively. The B/B' pair of peaks describes the redox process of *para*-aminodiphenylamine, a side product of PANI polymerization.¹⁵

An additional current peak E appears at the potential corresponding to the OPDA-monomer oxidation. While aniline monomer oxidation starts at ca. 750 mV,¹⁶ the oxidation potential of OPDA monomer starts at ca. 600 mV, because of the additional group in *ortho*-position.

A pair of D/D' peaks, not shown during polymerization of pure aniline solution, most probably represents a redox process of a new species originating from OPDA. As the polymer layer is transferred into the pure supporting electrolyte solution, the D/D' pair diminishes during the potential cycling. This implies that the species corresponding to the pair of D/D' peaks are of a low molecular weight, which has been occluded within the polymer layer. During the synthesis, a reddish-brown cloud, visible by the naked eye, appears around the working electrode. This might be due to the presence of radical species that are often colored or as side product in polymer-

ization of the OPDA monomer. Because the cloud expands within the solution and lasts even after the polymerization terminates, it appears to be a low molecular weight side product.

The polymer growing rate can be obtained from current value changes vs. number of synthesis cycles. In all the experiments, the growing rate slows down as the content of OPDA increases [Fig. 2(a-d)]. However, the influence of the switching potential, E_λ , and of aniline concentration, is also very pronounced. As expected,^{16,17} the rate of polymer layer growth increases as E_λ increases and as the concentration of aniline (An) monomer increases.

Figure 3 shows that, during polymerization from the mixture of aniline and OPDA, a current peak characteristic of poly-OPDA^{11,18,19} ($E_p \approx -100$ mV, current peak F) is obtained at the very beginning of the synthesis (2nd cycle), while PANI peaks were not yet registered. That proves that poly-OPDA is the first layer formed, which is clearly visible as a new current peak in the inset of Figure 3. Such behavior may be attributed to the OPDA lower oxidation potential. However, it can also be the consequence of the prevailing OPDA monomers in the coverage of the electrode due to the preferred competitive adsorption. Therefore, phenazine-like products¹⁴ (OPDA products) will prevail around the electrode at the beginning of synthesis. According to the literature,²⁰ the products of different molecular

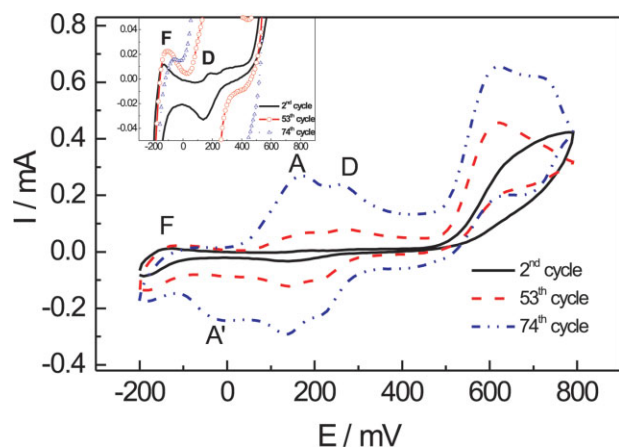


Figure 3 Current peak of poly-OPDA registered at the beginning of the polymerization process. [Color figure can be viewed in the online issue, which is available at www.interscience.wiley.com.]

mass surround the electrode during the polymerization process, and as they reach a critical mass, they precipitate on the electrode surface. Therefore, it is reasonable to assume that poly-OPDA is obtained as the first layer on the electrode surface. However, as the synthesis progresses, the OPDA concentration around the electrode decreases, and current peaks of the PANI redox process continue to increase and overlap the poly-OPDA current peak (74th cycle, Fig. 3).

Because the oxidation of aniline, as a prerequisite for polymerization, starts at ca. 750 mV, higher switching potential ($E_{\lambda} = 1000$ mV) ensures a much broader potential region available for aniline oxidation, favoring the polymerization of PANI over poly-OPDA, and the ratio of poly-OPDA to PANI is shifted toward PANI (i.e., the predetermined current value of peak A is achieved within a shorter time [Fig. 2(a–d)]). Considering different aniline concentrations, it follows that the influence of OPDA in a slowdown of the polymerization process is, as expected, much better pronounced in case of a lower concentration of aniline [Fig. 2(a–d)]. The influence of OPDA at different E_{λ} and at different aniline con-

centration, is well illustrated in Table I, which gives a relative number of cycles necessary to reach the value of 1.2 mA for current peak A. Some data in Table I are omitted because the influence of OPDA is negligible ($(N_{\text{PANI-OPDA}}/N_{\text{PANI}}) \approx 1$) or the synthesis of poly-OPDA lasts very long (*).

EIS measurements were done for PANI1 and PANI1-OPDA5 layers, because the influence of OPDA in this case was significant in slowing down the growth rate [Fig. 2(a)]. Both layers exhibit a pure capacitive behavior and show the same pseudo-capacitance value of 0.10 F cm^{-2} in the potential range of emeraldine [Fig. 4(a)]. The pseudo-capacitance reflects bulk properties of the polymer but not the interface properties. Because emeraldine prevails within the layers (i.e., within a bulk), similar capacitance values are obtained for both layers. It was not possible to determine the polymer resistance to characterize neither the metal/polymer nor the polymer/solution interface.^{21,22}

However, the measurements performed in the potential range of leucoemeraldine show the difference between these two layers as illustrated in Bode diagram [Fig. 4(b)]. A more detailed study is required to describe each of the elements of the applied electrochemical equivalent circuit (Table II). However, the obtained high resistances of R_1 and R_2 are characteristic of a nonconductive polymer layer. In the literature, it usually includes resistance of polymer layer, and resistance of pores within the polymer that are filled with electrolyte.^{23,24} Because PANI1-OPDA5 shows higher resistance values compared to PANI1, the size of pores and the amount of the solution within the pores should therefore be smaller in the case of PANI1-OPDA5 (i.e., the layer is more compact). The pseudo-capacitive values, Q_3 , at the potential of leucoemeraldine, for both of these layers, are different and significantly lower compared to the values of emeraldine state. However, a higher Q_3 value is obtained for PANI1 compared to PANI1-OPDA5. Finally, considering EIS measurements, it is clear that structurally different polymer material is obtained depending on the feed solution mixture.

TABLE I
Influence of OPDA Additions on the Polymer Layer Growth Presented as a Relative Number of Cycles ($N_{\text{PANI-OPDA}}/N_{\text{PANI}}$) Necessary to Reach the Current Value of 1.2 mA for Peak A in the Case of PANI and PANI-OPDA

OPDA concentration (mmol dm^{-3})	$N_{\text{PANI1-OPDA}}/N_{\text{PANI1}}$ 800 mV	$N_{\text{PANI2-OPDA}}/N_{\text{PANI2}}$ 1000 mV	$N_{\text{PANI3-OPDA}}/N_{\text{PANI3}}$ 800 mV	$N_{\text{PANI4-OPDA}}/N_{\text{PANI4}}$ 1000 mV
1	2.1	1.2	≈ 1	≈ 1
5	6.3	3.5	1.4	1.0
10	*	10.2	2.6	1.5
50	*	*	4.8	15.0

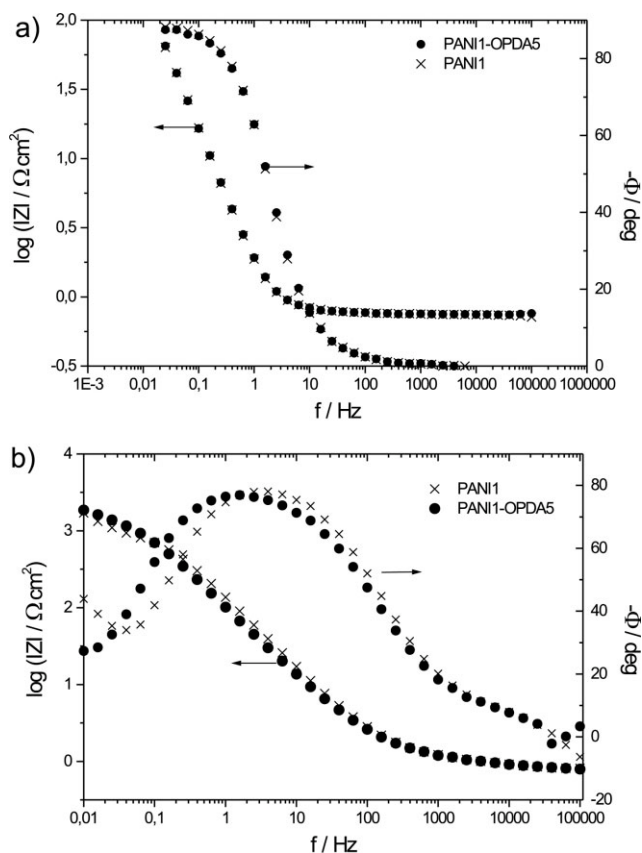


Figure 4 Bode diagrams for PANI1 and PANI1-OPDA5 layers polarized at (a) 400 mV and (b) -100 mV.

It was expected that different structures, as shown by EIS, should also result in a different number of "active" bipolaron centers on the polymer, necessary for the catalysis of H_2Q/Q quasi-reversible redox reaction. As shown by Matveeva,⁵ the catalytic effect of PANI depends on the sites available for the adsorption of H_2Q species on the protonated active centers of EM. Figure 5(a) illustrates RDE voltammograms of PANI1 and PANI1-OPDA layers and the bare Pt electrode. However, comparison with the

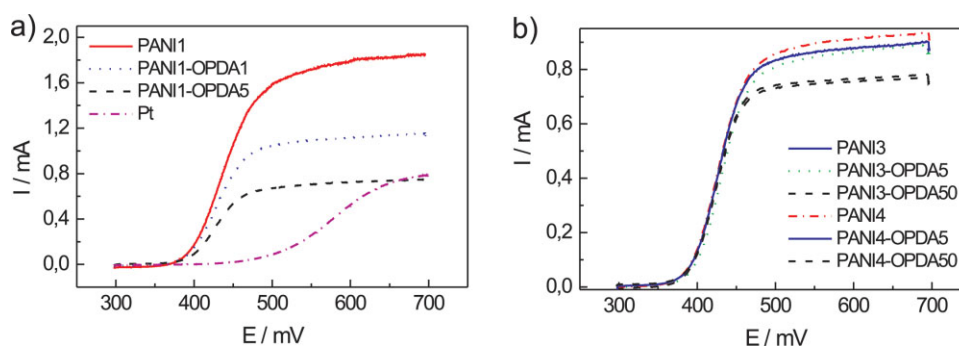


Figure 5 RDE voltammograms of H_2Q oxidation on electrodes coated with (a) different PANI1 layers synthesized from $c_{(An)} = 0.1 \text{ mol dm}^{-3}$ solutions, $\omega = 3000 \text{ min}^{-1}$, (b) different PANI3 and PANI4 layers synthesized from $c_{(An)} = 0.5 \text{ mol dm}^{-3}$ solutions, $\omega = 3000 \text{ min}^{-1}$. [Color figure can be viewed in the online issue, which is available at www.interscience.wiley.com.]

TABLE II
Results of Fitting the Impedance Data in Figure 7(b) to the Electrical Equivalent Circuit: $R_{sol}(Q_1(R_1(Q_2(R_2Q_3))))$

	PANI1	PANI1-OPDA5
$R_{sol} (\Omega)$	12.24	12.18
$Q_1 \times 10^4 (\Omega^{-1} \text{ s}^n \text{ cm}^{-2})$	4.09	5.70
n_1	0.91	0.88
$R_1 \times 10^{-4} (\Omega \text{ cm}^2)$	0.96	0.99
$Q_2 \times 10^4 (\Omega^{-1} \text{ s}^n \text{ cm}^{-2})$	9.21	13.14
n_2	0.91	0.88
$R_2 \times 10^{-3} (\Omega \text{ cm}^2)$	1.04	1.85
$Q_3 \times 10^3 (\Omega^{-1} \text{ s}^n \text{ cm}^{-2})$	7.42	1.38
n_3	0.78	0.72

n_1 , n_2 , and n_3 indicate the capacitor-like behavior of the constant phase elements Q_1 , Q_2 , and Q_3 . The impedance of the constant phase element is $Z_Q = A(j\omega)^{-n}$, where $0 < n < 1$, when $n = 1$ Q is considered to be a pure capacitor, A is the frequency independent constant, ω is the angular frequency, j is an imaginary unit, and R_{sol} is a solution resistance.

reaction at the bare Pt-electrode shows for all the polymer layers that there is a catalytic shift of H_2Q oxidation reaction to lower potentials. The transients obtained exhibit a similar behavior as those obtained earlier,¹⁰ but the limiting current values are lower than in the case of HCl supporting electrolyte. This indicates that the layers synthesized in a phosphoric acid solution result in a denser state, which offers a lower number of active sites for the catalytic reaction. As expected, the highest limiting current value is obtained in the case of pure PANI layer and as the OPDA additions increase, a decrease in the limiting current is registered. It is fair to assume that the current decrease is associated with the change of the layer morphology caused by the presence of OPDA (i.e., a more compact layer is produced, which leaves a lower number of active centers available for the H_2Q/Q reaction to take place). Such results are in agreement with the results obtained by EIS measurements.

Figure 5(b) illustrates RDE voltammograms for PANI3 and PANI4 layers. The concentration of 50

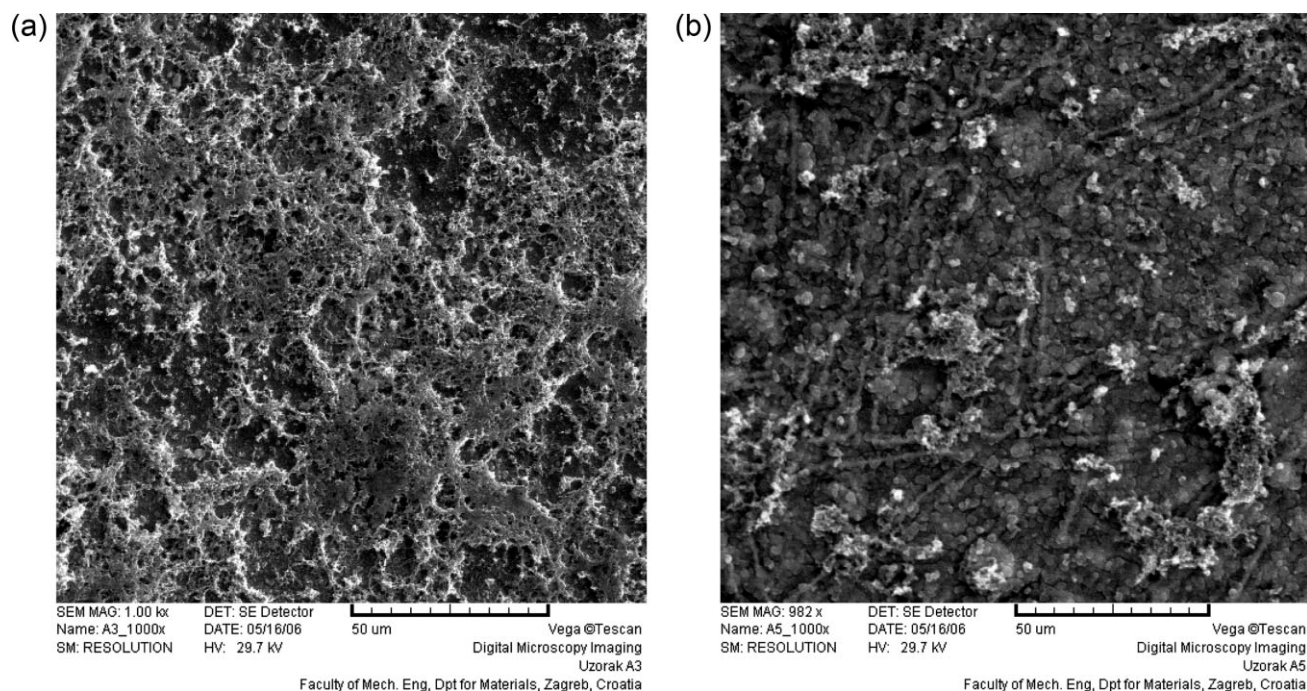


Figure 6 SEM micrographs of different layers synthesized from solutions of $c_{(\text{An})} = 0.1 \text{ mol dm}^{-3}$ at $E_{\lambda} = 800 \text{ mV}$: (a) PANI1 layer and (b) PANI1-OPDA5 layer.

mmol dm^{-3} OPDA influences the decrease of the limiting current. Nevertheless, in the case of the higher concentration of aniline, a more compact layer is formed,¹⁵ thus affecting the catalyses in the same manner as OPDA addition (i.e., by lowering the limiting currents [Fig. 5(a,b)]). Hence, the effect of OPDA addition is less pronounced in the case of PANI3 and PANI4 layers compared to PANI1 and PANI2 layers. The obtained higher density of PANI layer in the case of higher aniline concentration is the result of generated radical cations at the higher rate. Because radical cations initiate polymerization,^{20,25,26} a higher number of nucleation sites are expected in the solution surrounding the electrode surface. Because of the increased aniline concentration, a denser layer is obtained. Therefore, as Figure 5(b) shows, the increase in switching potential, E_{λ} (from 800 to 1000 mV), has practically no effect on the limiting current in the case of 0.5 mol dm^{-3} aniline.

The SEM micrographs taken for PANI1 show a sponge-like morphology with evident branching of polymer [Fig. 6(a)]. As illustrated in Figure 6(b), the concentration of 5 mmol dm^{-3} of OPDA in the feed solution results in a more compact PANI1-OPDA5 layer with less discernible fibers. The more compact structure of pure PANI2 over PANI1 layer because of higher E_{λ} is confirmed by Figure 7(a). Additional layer compactness is obtained with the concentration of 10 mmol dm^{-3} of OPDA (PANI2-OPDA10) [Fig.

7(b)]. The influence of aniline concentration on polymer morphology is evident from the comparison of Figure 7(a) and 7(c).

The increase of layer density due to the OPDA addition is shown by SEM micrographs, which supports the conclusion of RDE voltammetry. The EIS measurements also support the differences between these two layers. This method of tailoring the polymer layer density may be applied in corrosion protection of steel in an aggressive (e.g., chloride) medium, assuming reasonably that the increase of the layer density is instrumental in suppressing the ingress of aggressive Cl^{-} species through the protective polymer layer.

Stainless steel substrate

Considering the results obtained on the increase of polymer layer density, the effect of OPDA addition was also tested in the case of the polymer layer grown on an SS electrode. It was shown earlier⁴ that a PANI layer synthesized from 3 mol dm^{-3} H_3PO_4 solution protects SS from corrosion in an acidic medium, but the corrosion protection in the presence of Cl^{-} failed. It was also shown that a PANI layer synthesized from 1.5 mol dm^{-3} H_2SO_4 medium offers a short-time corrosion protection, which is improved by adding OPDA into the feed solution.²⁷ Assuming that the addition of OPDA into the feed solution for PANI synthesis in a phosphoric acid solution would

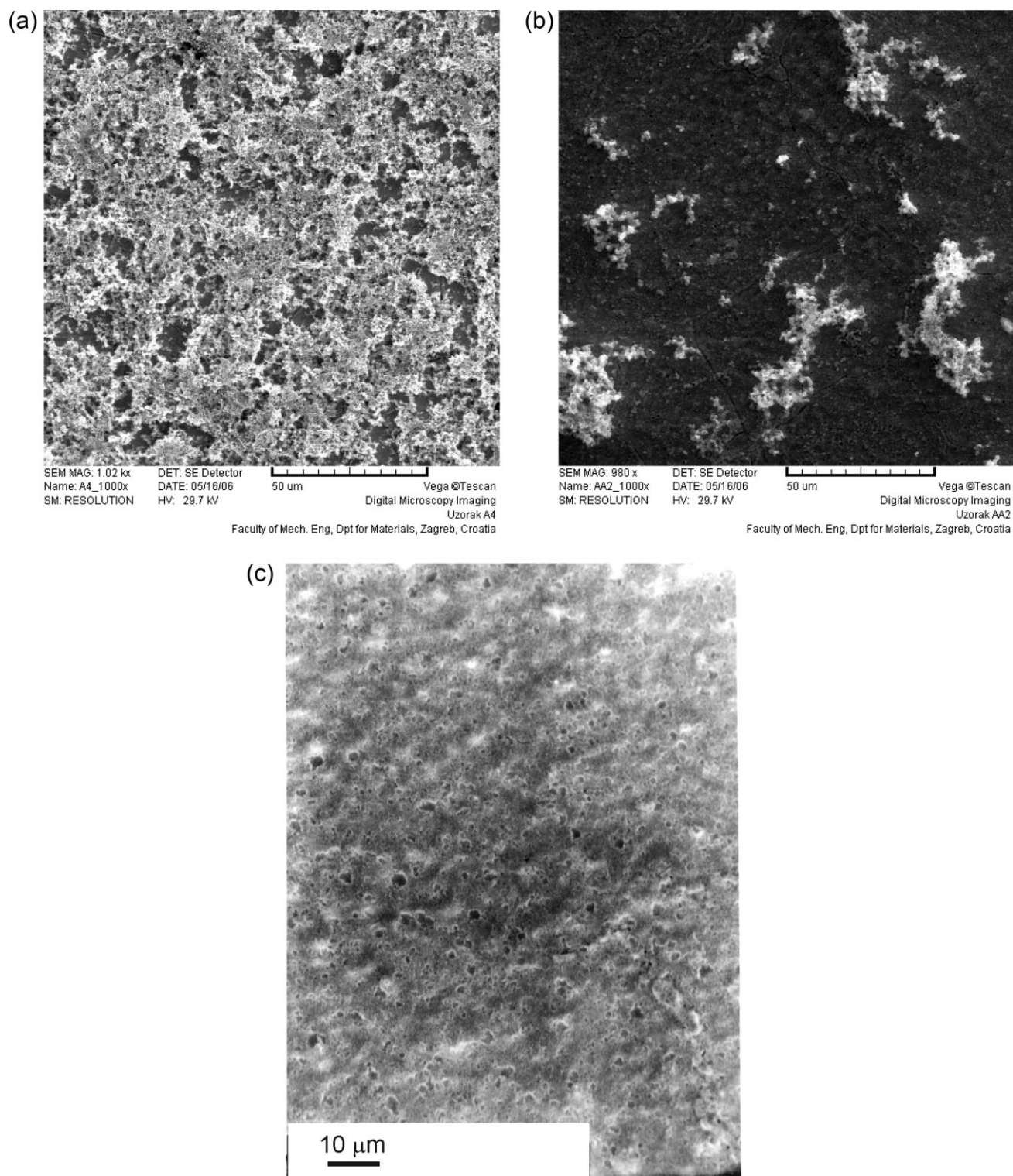
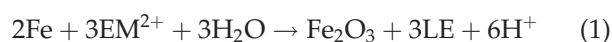


Figure 7 SEM micrographs of different layers synthesized from solutions of $c_{(AN)} = 0.1 \text{ mol dm}^{-3}$ at $E_\lambda = 1000 \text{ mV}$: (a) PANI2 layer, (b) PANI2-OPDA10 layer, (c) from solutions of $c_{(AN)} = 0.5 \text{ mol dm}^{-3}$ at $E_\lambda = 1000 \text{ mV}$, PANI4 layer.

also contribute to increased layer density, it was applied on a SS substrate.

The electrochemical mechanism of steel corrosion protection by PANI is explained through the formation of an oxide film on SS, followed by the simulta-

neous reduction of EM to LE.^{28,29} It is suggested that under open-air conditions, LE instantly converts back to EM according to the following reactions:



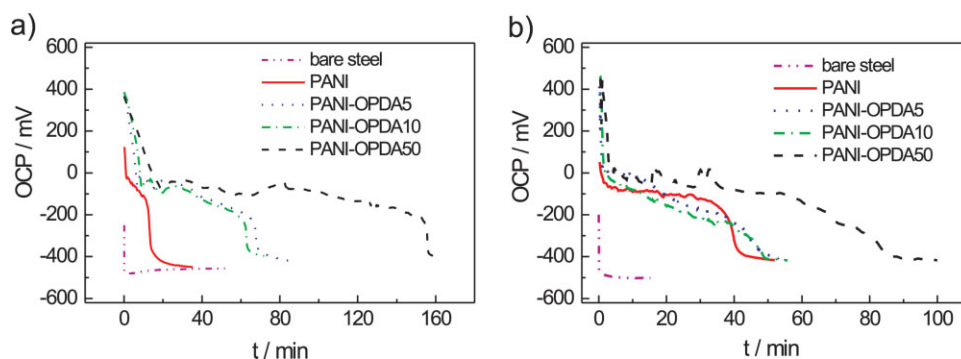


Figure 8 The OCP-time dependence for the bare stainless steel and stainless steel coated with different modified PANI layers ($c_{\text{OPDA}} = 0, 5, 10, \text{ and } 50 \text{ mol dm}^{-3}$) in (a) $3 \text{ mol dm}^{-3} \text{ H}_3\text{PO}_4 + 0.1 \text{ mol dm}^{-3} \text{ NaCl}$, (b) $0.1 \text{ mol dm}^{-3} \text{ HCl}$. [Color figure can be viewed in the online issue, which is available at www.interscience.wiley.com.]



Since SS, coated with a PANI layer, exhibits OCP in the potential region of EM, which overlaps with SS passive region, PANI corrosion protection property is explained through the “chemical potentiostat”³⁰ behavior (reactions 1 and 2). However, that protection mechanism does not operate in the presence of aggressive chloride ions.

Thus, monitoring of OCP vs. time enables the determination of the effect of PANI structure modified with OPDA on corrosion protection of SS. Figure 8(a,b) illustrates OCP vs. time dependence for SS coated with PANI layers containing different OPDA additions. The PANI-coated SS electrode, while

immersed in pure $3 \text{ mol dm}^{-3} \text{ H}_3\text{PO}_4$ supporting electrolyte, maintains the OCP in the potential range of EM, which is within the passive range of SS.⁴ In the case of Cl^- presence in the solution, the time of maintaining OCP, before falling into the active corrosion region, depends on the concentration of OPDA in the solution of synthesis (i.e., the protection time increases with the increase of OPDA concentration). These results confirm that OPDA addition changes polymer layer structure to a denser one compared to pure PANI. Therefore, the PANI-modified layer, apart from exhibiting the electrochemical mechanism of protection through reactions 1 and 2, has mainly the role of a physical barrier to the ingress of Cl^- ions toward the steel electrode

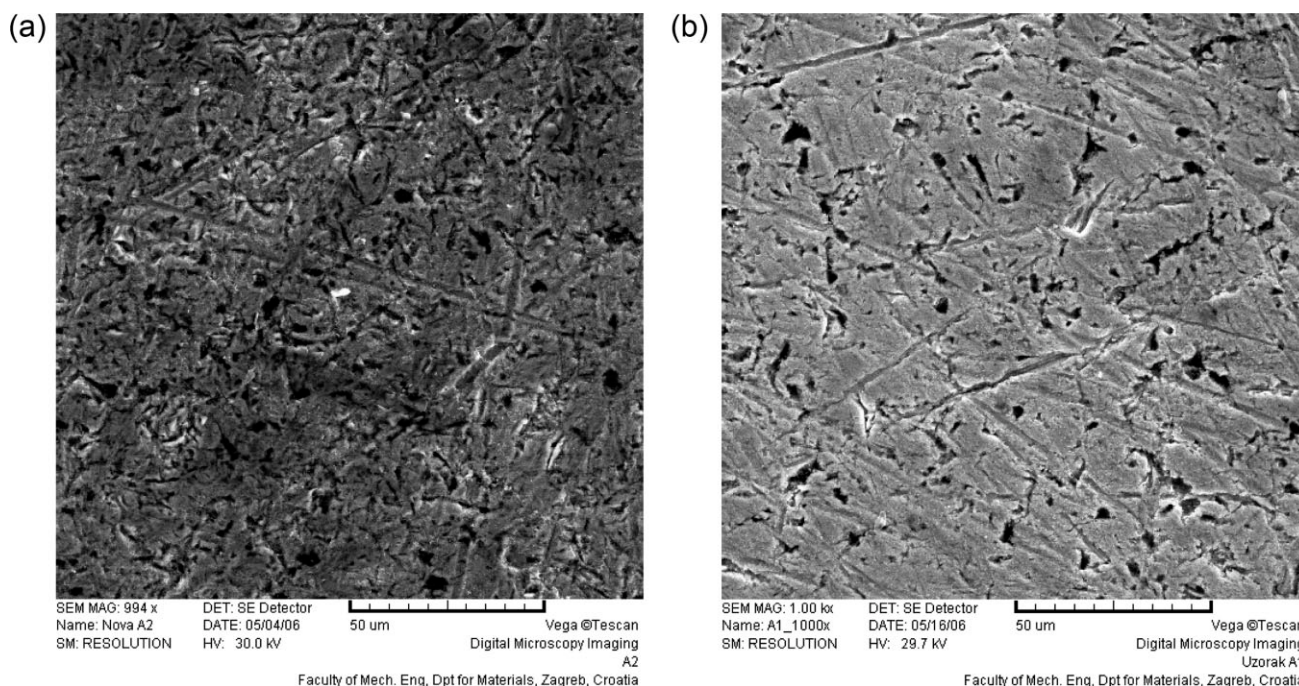


Figure 9 SEM micrographs for different layers synthesized on SS from solutions of $c_{\text{Ar}} = 0.5 \text{ mol dm}^{-3}$ at $E_{\lambda} = 1000 \text{ mV}$: (a) PANI layer, (b) PANI-OPDA50 layer.

substrate. SEM micrographs [Fig. 9(a,b)] illustrate the effect of OPDA additions on the morphology of the obtained polymer layers on the SS substrate. Because the protection time is increased, it follows that the increased density of the polymer layer makes the ingress of Cl^- ions more difficult.

It is worth noting that the protection lasts longer if Cl^- ions are added into the H_3PO_4 supporting electrolyte solution, compared to the protection time in pure 0.1 mol dm^{-3} HCl solution. One of the reasons for the better protection obtained in the presence of phosphate ions is the fact that phosphate ions support the repassivation of steel³¹ and thus help the oxide stability in the aggressive chloride environment. The reason for shorter protection times in pure HCl solution might be that the exchange of phosphate ions (and phosphate counter-ions) within the polymer layer with Cl^- ions is facilitated due to the absence of phosphate ions in the supporting electrolyte solution.

Therefore, the protection against corrosion caused by Cl^- ions is not of an electrochemical nature, but rather the result of the changed polymer layer density, which thus exhibits a physical barrier to Cl^- ions ingress through the polymer. Similar results were obtained by achieving dense morphology of the layer through the deprotonation of PANI.³²

CONCLUSIONS

The results of these investigations confirm that the addition of OPDA monomer to aniline polymerization solution slows down the polymerization rate and results in a more compact polymer layer compared to pure aniline solution, meaning that by administering a predetermined concentration of OPDA, the morphology of the resulting polymer may be tailored. The influence of OPDA addition is more pronounced at lower switching potentials and at lower aniline concentrations, due to the favored polymerization of OPDA, which takes place at lower potentials than aniline.

The different densities between layers are shown by SEM micrographs, by the decrease of the limiting current for $\text{H}_2\text{Q}/\text{Q}$ reaction, and by EIS measurements.

EIS measurements, at the potential range of leucoemeraldine, indicate differences in resistance between PANI1 and PANI1-OPDA5 layers as a result of a more compact PANI1-OPDA5 layer.

It is shown that it is possible to synthesize PANI layer and PANI modified with OPDA on SS electrode. In chloride solutions, a deceleration of chloride ions ingress through the PANI-OPDA polymer layer is established. This is attributed to the compact morphology of the layer, which acts as a physical

barrier to the ingress of Cl^- ions into the polymer layer, improving the corrosion protection of steel. Thus, the modified PANI layer acts not only as a "chemical potentiostat" but also as a physical barrier to the ingress of chloride ions.

NOMENCLATURE

An	Aniline
ω	Rotation speed, min^{-1}
Φ	Phase angle, deg
ν	Scan rate, V s^{-1}
E	Potential, V
EIS	Electrochemical impedance spectroscopy
EM	Emeraldine form of polyaniline
f	Frequency, Hz
I	Current, A
LE	Leucoemeraldine form of polyaniline
N	Number of cycles
OCP	Open circuit potential
OPDA	<i>ortho</i> -phenylenediamine
PADPA	<i>para</i> -aminodiphenylamine
PANI	Polyaniline
PG	Pernigraniline
Q	Constant phase element, $\Omega^{-1} \text{ s}^n \text{ cm}^{-2}$
R	Resistance, Ω
RDE	Rotating disc electrode
t	Time, s
Z	Impedance, $\Omega \text{ cm}^2$

References

- MacDiarmid, A. G.; Yang, L. S.; Huang, W. S.; Humphrey, B. D. *Synth Met* 1987, 18, 393.
- DeBerry, D. W. *J Electrochem Soc* 1985, 132, 1022.
- Santos, J. R., Jr.; Mattoso, L. H. C.; Matheo, A. J. *Electrochim Acta* 1998, 43, 309.
- Kraljić, M.; Mandić, Z.; Duić, Lj. *Corr Sci* 2003, 45, 181.
- Matveeva, E. S. *Synth Met* 1996, 83, 89.
- Mandić, Z.; Duić, Lj. *J Electroanal Chem* 1996, 404, 133.
- Malinauskas, A.; Garjonyte, R.; Mažeikiene, R.; Jurevičiute, I. *Talanta* 2004, 64, 121.
- Sanchís, C.; Salavagione, H. J.; Arias-Pardilla, J.; Morallón, E. *Electrochim Acta* 2007, 52, 2978.
- Li, M.; Jing, L. *Electrochim Acta* 2007, 52, 3250.
- Duić, Lj.; Kraljić, M.; Grigić, S. *J Polym Sci* 2004, 42, 1599.
- Malinauskas, A.; Bron, M.; Holze, R. *Synth Met* 1998, 92, 127.
- Mažeikiene, R.; Malinauskas, A. *React Funct Polym* 2000, 45, 45.
- Prokeš, J.; Stejskal, J.; Křivka, I.; Tobolková, E. *Synth Met* 1999, 102, 1205.
- Xiang, C.; Xie, Q.; Hu, J.; Yao, S. *Synth Met* 2006, 156, 444.
- Yang, H.; Bard, A. J. *J Electrochem Soc* 1992, 339, 423.
- Duić, Lj.; Mandić, Z.; Kovač, S. *Electrochim Acta* 1995, 40, 1681.
- Duić, Lj.; Grigić, S. *Polimeri* 1997, 18, 176.
- Levi, M. D.; Pisarevskaya, E. Yu. *Electrochim Acta* 1992, 37, 635.

19. Puskás, Z.; Inzelt, G. *Electrochim Acta* 2005, 50, 1418.
20. Bade, K.; Tsakova, V.; Schultze, J. W. *Electrochim Acta* 1992, 37, 2255.
21. Horvat-Radošević, V.; Kvastek, K.; Kraljić Roković, M. *Electrochim Acta* 2006, 51, 3417.
22. Ferloni, P.; Mastragostino, M.; Meneghello, L. *Electrochim Acta* 1996, 41, 27.
23. Roßberg, K.; Paasch, G.; Dunsch, L.; Ludwig, S. *J Electroanal Chem* 1998, 443, 49.
24. Fiorit, M. I.; Posadas, D.; Molina, F. V.; Andrade, E. M. *J Electrochem Soc* 1999, 146, 2592.
25. Andrade, G. T.; Aguirre, M. J.; Biaggio, S. R. *Electrochim Acta* 1998, 44, 633.
26. Duić, Lj. In *Polymeric Materials Encyclopedia, Polyaniline (Electrochemical Synthesis)*; Salamone, J. C., Ed.; CRC Press: Boca Raton, 1996; Vol. 7, p 5489.
27. Kraljić, M.; Žic, M.; Duić, Lj. *Bull Electrochem* 2004, 20, 567.
28. Wessling, B. *Synth Met* 1997, 85, 1313.
29. Bernard, M. C.; Joiret, S.; Hugot-Le Goff, A.; Long, P. D. *J Electrochem Soc* 2001, 148, B299.
30. Bernard, M. C.; Joiret, S.; Hugot-Le Goff, A.; Phong, P. V. *J Electrochem Soc* 2001, 148, B12.
31. Lakatos-Varsányi, M.; Falkenberg, F.; Olefjord, I. *Electrochim Acta* 1998, 43, 187.
32. Kraljić Roković, M.; Kalić, M.; Duić, Lj. *Chem Biochem Eng* 2007, 21, 59.